Available online at www.sciencedirect.com
SCIENCE DIRECT®
Journal of Solid State Chemistry 179 (2006) 1513–1520
JOURNAL OF SOLID STATE CHEMISTRY
www.elsevier.com/locate/jssc

A study of carboxylic-modified mesoporous silica in controlled delivery for drug famotidine

Qunli Tang[a,b], Yao Xu[a,*], Dong Wu[a], Yuhan Sun[a]

[a]State Key Laboratory of Coal Conversion, Institute of Coal Chemistry, Chinese Academy of Sciences, Taiyuan, Shanxi province 030001, PR China
[b]Graduate School of the Chinese Academy of Sciences, Beijing 100039, PR China

Received 15 October 2005; received in revised form 28 December 2005; accepted 4 February 2006
Available online 10 March 2006

Abstract

A series of pure silica MSU and carboxylic-modified MSU materials were prepared. The formation of mesoporous silica materials with terminal carboxylic groups on pore surface was performed by the acid-catalyzed hydrolysis of cyano to carboxylic. Then their potential applications in controlled drug delivery carriers were investigated. Drug famotidine was selected as a model molecule out of the consideration of the terminal amino groups in its molecule. The adsorption experiments show significant adsorption of famotidine on the carboxylic-modified MSU materials. And, the functionalization level of carboxylic groups has been found to be the key factor affecting the adsorption capacities of the modified MSU materials for famotidine. Subsequently, three kinds of release fluids, including simulated gastric medium, simulated intestinal medium, and simulated body fluid, were used to test the famotidine release rate from the carboxylic-modified MSU material. Obvious delayed effect has been observed for the famotidine release from the carboxylic-modified mesoporous silica material under the in vitro assays.

Keywords: Mesoporous material; MSU; Carboxylic-modified; Famotidine; Controlled drug delivery

1. Introduction

Porous silica materials employed as convenient drug reservoirs in controlled drug delivery have received much attention these years. Zeolites, typical microporous materials, have been investigated for use as carriers for a variety of drugs [1–3]. However, for the guest molecules of pharmaceutical interest, which are usually larger than 2 nm, zeolites are not appropriate to be used as carriers due to the relatively small pore size. Interestingly, the Mobil Oil Corporation discovered the M41s group of mesoporous materials in 1992 [4]. And then various kinds of mesoporous materials (such as SBA-15, MSU) have been successfully synthesized over the last few years [5,6]. Generally, mesoporous silica materials have very high specific surface areas and large pore volumes. These useful properties allow them to accept high amount of drug molecules. Moreover, mesoporous silica materials have tunable pore sizes ranging from 2 to several ten nanometers, and the pore sizes can be well adjusted by choosing appropriate surfactant template and reaction conditions, enlarging the applications of porous silica in hosting large guest molecules [7–11].

In 2001, Vallet-Regí and co-workers primarily reported the application of silica MCM-41 for controlled release of ibuprofen under the in vitro assays [12]. Afterwards, several research groups investigated the drug adsorption and release properties of mesoporous silica materials [13–22]. An ideal mesoporous carrier with high specific surface area, large pore volume, and appropriate pore size (larger than the kinetic diameter of drug) was beneficial to increasing its adsorption capacity for drug [14,16]. Ibuprofen, which contains a terminal carboxylic group, has been much documented [12–19]. Ibuprofen can be impregnated into mesoporous silica materials by reacting with the active groups on the mesoporous framework, for instance, by the hydrogen bond interaction with surface silanol groups [12,16], by the coulombic interaction with functional aminopropyl groups [13], and even through the ester

*Corresponding author. Fax: +86 351 4041153.
E-mail addresses: xuyao@sxicc.ac.cn (Y. Xu), yhsun@sxicc.ac.cn (Y. Sun).

0022-4596/$ - see front matter © 2006 Elsevier Inc. All rights reserved.
doi:10.1016/j.jssc.2006.02.004

function with the epoxide ring opening of glycidoxypropyl [15]. As yet, to the best of our knowledge, how to apply mesoporous silica carrier system to impregnate a new kind of model drug molecule for controlled delivery is of keen interest.

Herein, famotidine was selected as a model drug molecule. Different from ibuprofen molecule containing a terminal carboxylic group, famotidine molecule contains terminal amino groups. In addition, famotidine has two well-known crystal structural dimensions of 1.7862 nm × 0.5329 nm × 1.8307 nm (molecular volume of 1.4431 nm^3) and 1.1978 nm × 0.7196 nm × 1.6812 nm (molecular volume of 1.4281 nm^3) [23], making it very appropriate to be impregnated into the pore channels of mesoporous materials. In our previous work [24], a preliminary result was reported about the effective adsorption of the carboxylic-modified mesoporous silica SBA-15 materials for drug famotidine. It has been found that the adsorption for famotidine depends strongly on the functionalization levels of carboxylic incorporated on the pore surface the modified mesoporous SBA-15 materials. Also, the impregnated amount of famotidine was affected by the adsorption experimental conditions, including pH value, solvent nature and initial famotidine concentration in the impregnation mixture. The purpose of this work was to obtain further controlled famotidine release from the carboxylic-modified mesoporous silica materials. MSU-type mesoporous silica materials modified by carboxylic groups were investigated as drug carriers. The characterization of the mesoporous silica materials and their adsorption and release properties for famotidine were described in detail.

2. Experimental section

2.1. Materials

The starting materials employed in this study were tetraethoxysilane (TEOS, 99%, TSR), surfactant $C_{11-15}H_{22-30}(CH_2CH_2O)_9H$ (AEO_9, HenKel), 2-cyanopropyltriethoxysilane (CPTES, 95%, Aldrich), sulfuric acid (H_2SO_4, 98%, SCR), methanol (CH_3OH, Anhydrous, SCR), ethanol (C_2H_5OH, Anhydrous, SCR), sodium fluoride (NaF, 99%, SCR) and famotidine ($C_8H_{15}N_7O_2S_3$, 99.9%, QDPF). All chemicals were used as received. The structural formula of famotidine is shown in Scheme 1.

2.2. Synthesis

The preparation of mesoporous silica materials was partially based on the previously published synthesis routes [25–29]. Typically, TEOS and CPTES were, separately, added to a stirring mixture of AEO_9 and H_2O at ambient temperature. After 30 min stirring, the regulated amount of NaF was added to the above mixture at a final molar composition: $(1-x)$TEOS:xCPTES:0.1AEO_9:0.027NaF:146H_2O, where x was designated as 0, 0.05, 0.15, 0.2. The mixture was stirred for 18 h, followed by heating at 50 °C for another 72 h without stirring. The resulting powers were filtered, air-dried and extracted by Soxhlet extraction with ethanol for 48 h. The obtained pure silica mesoporous material was designated as MSU, and the obtained cyanopropyl-modified mesoporous materials were designated as MSU-1_{CN}, MSU-2_{CN} and MSU-3_{CN} corresponding to the products synthesized with the x of 0.05, 0.15 and 0.20, respectively. The conversion of cyano to carboxylic, based on the reported procedure [28,29], was performed by adding 1.0 g of the cyanopropyl-modified mesoporous silica in 120 mL of 60% (v/v) aqueous sulfuric acid with stirring for 3 h at 150 °C. The treated sample was washed with copious amounts of water and then dried at 100 °C. The resulting products were labeled as MSU-1, MSU-2 and MSU-3 corresponding to MSU-1_{CN}, MSU-2_{CN} and MSU-3_{CN}, respectively.

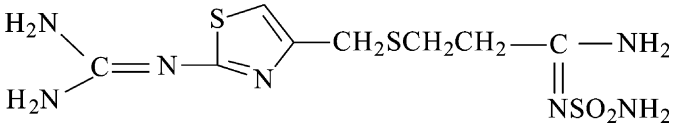

Scheme 1. Structural formula of famotidine.

2.3. Impregnation

Famotidine was dissolved in 50% (v/v) aqueous methanol solution with famotidine concentration C_0 and labeled as solution A. Then, 1.0 g of the powder mesoporous silica material was soaked in 1000 mL of solution A. The pH of the mixture was adjusted to 7.0 by adding 2.0 mol/L aqueous hydrochloric acid. Then the above mixture was stirred gently for 4 h at ambient temperature. The obtained famotidine-impregnated mesoporous silica was separated via filtrating. The impregnated amount of famotidine was assessed by subtracting the amount of famotidine remained in the aqueous methanol solution from the total amount of famotidine added. The famotidine content remained in the solution was measured by UV/vis spectrophotometer at a wavelength of 286 nm. The sample number of MSU-3 + famo is corresponding to the product obtained by adding the MSU-3 in the famotidine solution with the initial famotidine concentration C_0 at 2.0 mg/mL.

2.4. Release

In vitro release of famotidine was studied in three different kinds of release fluids, including simulated gastric medium (HCl aqueous solution, pH = 1.3), simulated intestinal medium (phosphate buffer solution, pH = 7.4) and simulated body fluid (SBF, pH = 7.4). The SBF has an ionic composition similar to the human body plasma (pmm: $Na^+/K^+/Ca^{2+}/Mg^{2+}/Cl^-/HCO_3^-/HPO_4^{2-}/SO_4^{2-}$ of 142.0/5.0/2.5/1.5/147.8/4.2/1.0/0.5) [30]. In a typical case, 0.3 g of the MSU-3 + famo was compressed to get a disk by uniaxial pressure (3 MPa). The cross section and thickness of the disk was about 12 and 3 mm, respectively. Then the

disk was soaked in 900 mL of release fluid at 37 °C under continuous stirring at a rate of 100 rpm. The release fluid (5 mL) was removed for analysis at given time intervals, and replaced with 5 mL of fresh release fluid. For the sake of comparison, the dissolution profiles of famotidine, have been investigated by adding 0.05 g of famotidine in 900 mL of solution at 37 °C under continuous stirring at a rate of 100 rpm. The sample number of MSU-3-famo is corresponding to the final solid after the release of the impregnated famotidine from the MSU-3 + famo in SBF.

2.5. Characterization

Powder XRD patterns were collected on a on a Rigaku diffractometer using Cu$K\alpha$ radiation. Nitrogen adsorption measurement was performed on a Micromeritics Tristar 3000 sorptometer at liquid nitrogen temperature. The specific surface area was calculated using the multiple-point Brunauer–Emmett–Teller (BET) method. The pore size distribution curve was calculated from the adsorption branch of the isotherm using the Barrett–Joyner–Halenda (BJH) method. Transmission electron microscopy (TEM) of samples was observed on a JEOL JEM-2010 electron microscope. Fourier transform infrared (FTIR) spectrum was obtained on a Nicolet Nexus 470 FT-IR analyzer using the KBr method. The famotidine concentration in solution was measured on a Shimadzu UV-2501PC UV spectrometer. The absorbance was measured at the wavelength of 266, 275 and 286 nm in simulated gastric medium, simulated intestinal medium, and SBF, respectively.

All ^{29}Si NMR experiments were performed at 9.4 T on a Varian Infinityplus-300 spectrometer using 7.5 mm probe under magic-angle spinning. The resonance frequency is 79.5 MHz. The 90° pulse width is measured to be 4.8 μs. Repetition time of 100 s for ^{29}Si single-pulse experiments was used.

3. Results and discussions

3.1. General features of the synthesized materials

The modified mesoporous materials possess XRD patterns with appearances typical of those of an MSU-type wormlike mesostructure, featuring a single peak at low 2θ angles usually between 1° and 3° [25,26]. The d_{100} spacings decrease from 7.36 to 6.17 nm with enhancing the molar ratio of CPTES/(CPTES + TEOS) in the initial synthesis mixture (see Table 1). Evidence for disordered, wormlike mesostructure in the modified samples is provided by typical transmission electron micrograph image (see Fig. 1a). As can be seen from the micrograph for the MSU-3 prepared with 20 mol% of CPTES/(CPTES + TEOS), which reveals typical wormlike packing of the pore channels.

The N_2 adsorption/desorption isotherms and pore size distribution curves of the modified MSU materials are displayed in Fig. 2, and the detailed pore textural parameters are summarized in Table 1. It is found that, for the MSU-1, MSU-2 and MSU-3, the N_2 isotherms show well-resolved inflexions at relative pressures between 0.3 and 0.4, demonstrating the existence of uniform

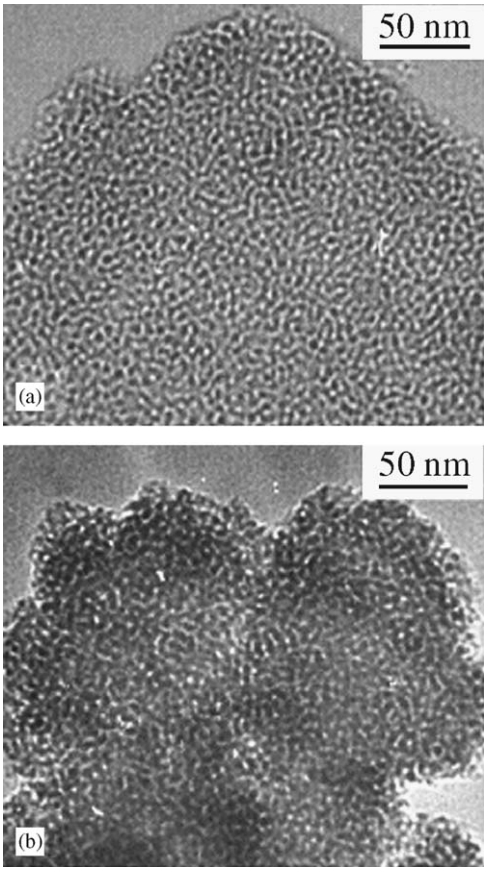

Fig. 1. TEM micrographs of: (a) MSU-3 and (b) MSU-3 + famo.

Table 1
Physical–chemical property for the related samples

Sample	d_{100} (nm)	Pore diameter[a] (nm)	BET surface area (m^2/g)	Pore volume (cm^3/g)
MSU-1	7.36	4.9	721	0.89
MSU-2	7.03	4.3	690	0.74
MSU-3	6.17	4.0	650	0.63
MSU-3 + famo	6.69	3.8	283	0.33
MSU-3-famo	6.84	3.8	583	0.51

[a]Pore diameter is pointed to the peak value in the pore size distribution.

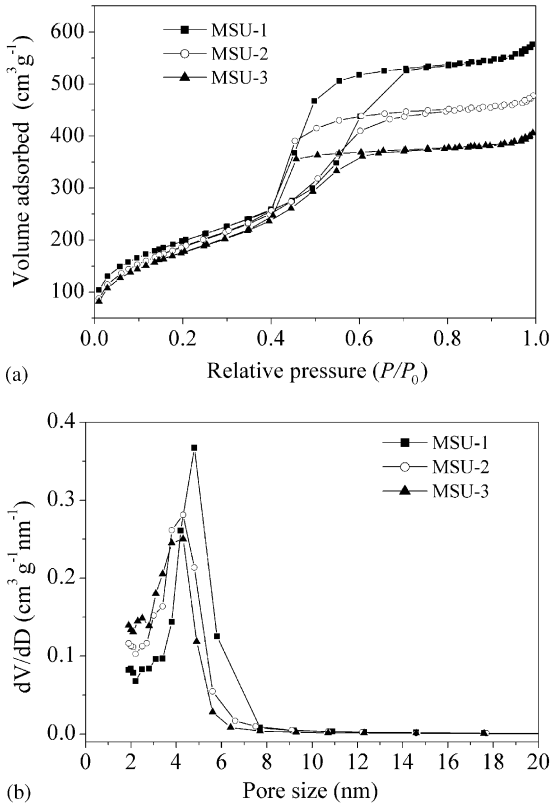

Fig. 2. (a) N_2 adsorption/desorption isotherms and (b) BJH pore size distribution curves of carboxylic-modified MSU materials.

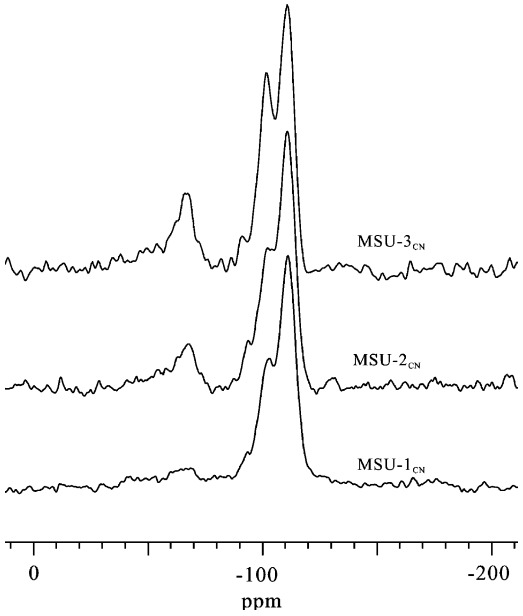

Fig. 3. ^{29}Si MAS NMR spectra of the related cyanopropyl-modified mesoporous silica materials.

Table 2
^{29}Si MAS NMR data for the related cyanopropyl-modified samples

Sample	δ (relative integrated intensity (%))					$T^n/(T^n+Q^n)$[a]
	Q^4	Q^3	Q^2	T^3	T^2	
MSU-1$_{CN}$	62.7	25.3	7.9	4.1	—	4.1
MSU-2$_{CN}$	54.0	28.4	5.0	8.3	4.3	12.6
MSU-3$_{CN}$	43.5	38.7	1.4	7.6	8.8	16.4

[a] $T^n = T^2 + T^3, Q^n = Q^2 + Q^3 + Q^4$.

mesoporous channels. Additionally, the modified samples show a pore size distribution typical for this type of wormlike mesoporous material. The pore sizes, pore volumes and specific BET surface areas of the modified samples are observed to be dependent on the molar ratio of CPTES/(CPTES + TEOS), and the pore textural parameters decrease with increasing molar ratio of CPTES/(CPTES + TEOS) in the synthesis mixture (see Table 1). The MSU-3 has a specific BET surface area of 650 m^2/g and pore volume of 0.63 cm^3/g, interestingly, which are only a little smaller than those obtained for the MSU-1 with a specific BET surface area of 721 m^2/g and pore volume of 0.89 cm^3/g. This result indicates that the MSU-3 prepared with the highest molar ratio of CPTES/(CPTES + TEOS) still has the well-defined mesostructure in comparison with the MSU-1.

The incorporation of cyanopropyl groups into the modified MSU materials was investigated by ^{29}Si MAS NMR (see Fig. 3). In the spectra of the samples, the three peaks appear at −111, −101, and −92 ppm, which can be assigned to Q^4, Q^3 and Q^2 species of the silica framework [$Q^n = Si(OSi)_n(OH)_{4-n}$, $n = 2$–4] [31–34]. Another two broader and partially overlapping signals due to organosiloxane units derived from CPTES are observed at the T^2 [$(SiO)_2Si$–$(CH_3)_2$] (−55 ppm) and T^3 [$(SiO)_3Si$–CH_3] (−65 ppm), respectively [33,34]. The emergence of the T^3 and T^2 peaks indicates the successful silylation. The ^{29}Si MAS NMR data are summarized in Table 2. The ratios of the $T^n/(T^n + Q^n)$ allow the quantitative assessment of the functionalization levels in the modified MSU materials. The grafted amounts of cyanopropyl groups in the MSU-1$_{CN}$, MSU-2$_{CN}$, and MSU-3$_{CN}$ are 4.1%, 12.6%, and 16.4% (related to the total silicon atoms), respectively. The higher molar ratio of CPTES/(CPTES + TEOS), the higher density of cyanopropyl groups in mesoporous silica materials.

Fig. 4 shows the FTIR spectra of the carboxylic groups modified MSU materials. In the FTIR spectra of the MSU-1, MSU-2, and MSU-3, the stretching vibration of cyano groups at 2253 cm^{-1} can hardly be observed while the strongly carboxylic stretching vibration at 1716 cm^{-1} appears, indicating a very high conversion of cyano groups to carboxylic groups.

3.2. Adsorption of famotidine

The adsorption of the carboxylic-modified MSU materials for famotidine was investigated by determining adsorption profiles from famotidine aqueous methanol

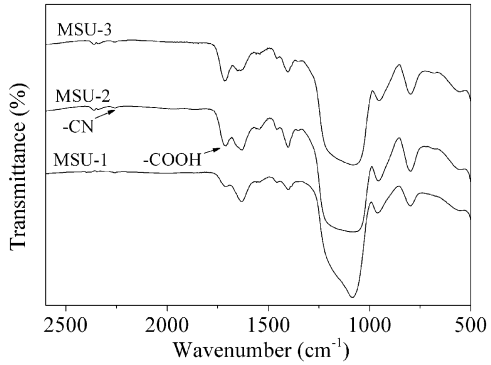

Fig. 4. FTIR spectra of the carboxylic-modified mesoporous silica materials.

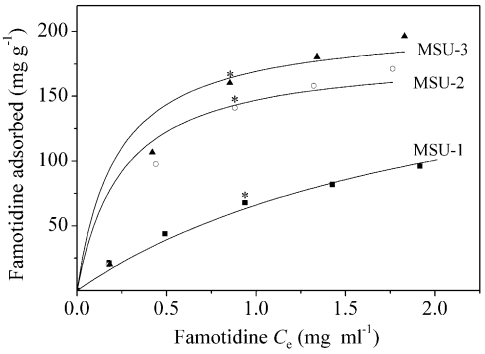

Fig. 5. Famotidine adsorption isotherms on the carboxylic-modified mesoporous silica materials from famotidine aqueous methanol co-solution.

co-solution. An impregnation time of 4 h was used and found to be sufficient to reach adsorption equilibrium. The adsorption profiles at ambient temperature are fitted using the Langmuir equation as follows:

$$Q_a = \frac{Q_m K C_e}{1 + K C_e}, \quad (1)$$

where Q_a is the amount of famotidine (in mg) adsorbed per gram weight of mesoporous solids, C_e is the equilibrium concentration of famotidine in the aqueous methanol solution, Q_m is the maximum adsorption capacity, and K is the constant.

Clearly, Fig. 5 shows large differences in adsorption capacities among the MSU-1, MSU-2 and MSU-3. The adsorption amounts of 67.7, 141.2 and 160.4 mg/g are obtained corresponding to the MSU-1, MSU-2 and MSU-3, respectively, under the same initial famotidine concentration of 1 mg/mL (labeled by the asterisks in Fig. 5). In addition, the maximum adsorption capacities (expressed as Q_m) of 155.52 ± 0.79, 307.92 ± 4.98 and 342.54 ± 0.32 mg/g are determined for the MSU-1, MSU-2, and MSU-3, respectively, according to Eq. (1) by fitting of the experimental data, as listed in Table 3. The differences in adsorption capacities among the carboxylic-modified MSU materials would be linked to the functionalization levels of carboxylic groups. Furthermore, it has been found that the amount of famotidine adsorbed into the MSU can even be neglected under the same adsorption conditions as mentioned above. Based on the above results, it can be confirmed that the incorporation of carboxylic groups into mesoporous silica provides the famotidine with a benign surrounding microenvironment. This fact is in good agreement with the observation mentioned in our previous paper, which revealed the pure silica SBA-15 could not adsorb any amount of famotidine [24]. Apparently, the adsorption for famotidine is the result of the interaction between the terminal carboxylic groups on the pore surface of the mesoporous materials and the famotidine molecules.

Table 3
The adsorption parameters determined according to Eq. (1) for the related carriers

Sample	Q_m	K	R^2
MSU-1	155.52 ± 0.79	0.81 ± 0.08	0.998
MSU-2	307.92 ± 4.98	0.79 ± 0.37	0.963
MSU-3	342.54 ± 0.32	0.82 ± 0.42	0.951

R^2 represents the correlation coefficient according to Eq. (1).

About the interaction between the carboxylic groups and the famotidine molecules, further evidence can be obtained by comparing the FTIR spectra of the samples MSU-3, MSU-3 + famo, and MSU-3-famo, as illustrated in Fig. 6. In the FTIR spectrum of the MSU-3 + famo, besides the carboxylic stretching vibration (1716 cm^{-1}) of low intensity is still observed, an intense carboxylate band at 1555 cm^{-1} is detected, suggesting that the COO^-–N^+ bondings have formed between the famotidine molecules and the carboxylic groups in the carboxylic-modified MSU materials. For the MSU-3-famo, the carboxylate vibration (1555 cm^{-1}) is weakened, simultaneously the carboxylic stretching vibration (1716 cm^{-1}) is enhanced, suggesting that major part of the carboxylic groups in the MSU-3 can be renewed after the release of famotidine.

Fig. 7 shows the N_2 adsorption/desorption results of the samples MSU-3, MSU-3 + famo, and MSU-3-famo. The detailed pore parameters are collected in Table 1. It can be seen the obvious decrease of the pore volume from 0.63 to 0.33 cm^3/g and the BET surface area from 650 to 283 m^2/g after the adsorption of famotidine into the MSU-3, demonstrating that famotidine molecules occupy part of the pore volume. As expected, after release of the adsorbed famotidine from the MSU-3 + famo in SBF, the pore volume and the BET surface area are almost recovered to the value before adsorption of famotidine.

In addition, MSU-3 + famo was studied by TEM (Fig. 1b). In comparison with the TEM image of MSU-3 (see Fig. 1a), it can be observed that there are no obvious differences in the TEM images between the MSU-3 and MSU-3 + famo. Moreover, the pore structure observed shows the MSU-3 + famo still remained the well-defined pore structure after the adsorption process for famotidine.

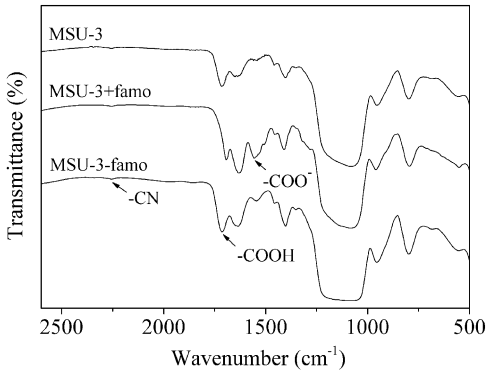

Fig. 6. FTIR spectra of samples MSU-3, MSU-3 + famo and MSU-3-famo.

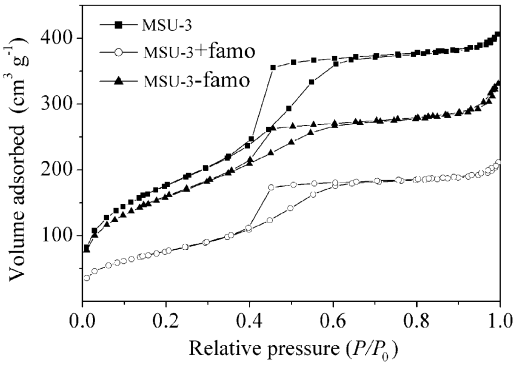

Fig. 7. N_2 adsorption/desorption isotherms of the related samples of MSU-3, MSU-3 + famo and MSU-3-famo.

3.3. Release of famotidine

The controlled release of active agents from an inert matrix has become increasingly important for oral, transdermal or implantable therapeutic systems, due to its advantages of safety, efficacy and patient convenience. Here, typical famotidine release profiles from the MSU-3 + famo were determined experimentally and were compared with the dissolution profiles of famotidine under the same conditions. In the experiments of determining the famotidine dissolution profiles, the final famotidine concentrations were prearranged at 0.056 mg/mL. This famotidine concentration is identical to that concentration resulted from the complete release of the adsorbed famotidine in the MSU-3 + famo.

The results of the famotidine release from the MSU-3 + famo are plotted in Fig. 8. Fig. 8a–c are corresponding to the release in the release solutions of simulated gastric medium, simulated intestinal medium, and SBF, respectively. The complete dissolution of famotidine needs 0.2, 0.5 and 1 h corresponding to the dissolution in the solutions of simulated gastric medium, simulated intestinal medium, and SBF, respectively. It clearly shows that the dissolution rate of famotidine is controlled by the pH of the solutions. The lower pH of the solution of simulated gastric

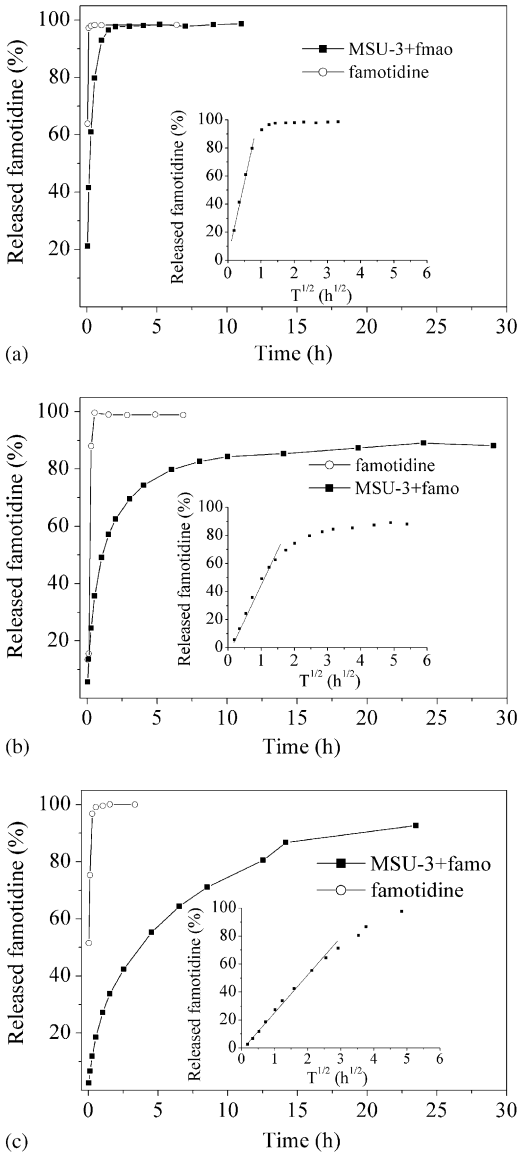

Fig. 8. Famotidine dissolution curves and famotidine release profiles from the MSU-3 + famo in the solutions of: (a) simulated gastric medium; (b) simulated intestinal medium; and (c) simulated body fluid. Inset: correlation of the percent of released famotidine vs. the square root of leaching time $t^{1/2}$.

medium results in the faster dissolution rate, due to the alkaline property of famotidine. For the solutions of simulated intestinal medium and SBF with the same initial pH of 7.4, the dissolution of famotidine leads to the enhancement of pH up to 7.58 in SBF, but cannot change the pH in simulated intestinal medium. Famotidine molecule contains the terminal $–NH_2$ groups, the dissolution of famotidine in SBF results in the formation of $–NH_3^+$ cations in the partial famotidine. Based on the ionic equilibrium, the concentration of OH^- enhances in SBF, consequently, resulting the enhancement of pH. Such a difference may be responsible for the difference of the dissolution rates in simulated intestinal medium and SBF. By comparing the famotidine release profiles from the

MSU-3 + famo with the dissolution profiles of famotidine, it can be concluded that strongly delayed effect is pressed on the famotidine release by the carboxylic-modified MSU material. The complete release of the adsorbed famotidine in simulated gastric medium needs almost 2 h of assay. The release of 80% of the adsorbed famotidine can be reached only after 6 and 13 h of assays in simulated intestinal medium and SBF, respectively. Interestingly, the same variation tendency, for the release rates of the adsorbed famotidine from the MSU-3 + famo and the dissolution rate of famotidine affected by the pH of solutions, is observed. Therefore, it should be noted that the own alkaline property of famotidine plays an important effect on its release rates in release solutions. The drug release process can be presumed as follows: before release of the drug can occur, the release fluid must penetrate into the pores and the adsorbed drug must dissolve into the permeating fluid then diffuse from the system. Obviously, the solution of simulated gastric medium with lower pH is beneficial to increasing the drug dissolution into the release media.

The delayed effect for the adsorbed famotidine release by the carboxylic-modified mesoporous silica carrier is very distinct. Firstly, the delayed effect can be ascribed to the use of the disk form of the MSU-3 + famo under the in vitro assays. For the powder MSU-3 + famo sample, the compression leads to a decrease of the material surface area available directly in the release solutions. As described in the above paragraph about the drug release process, obviously, the use of the disk form of the MSU-3 + famo can induce a slow release of famotidine due to the diffusion constraint by reduced surface area. Secondly, the COO^{-}–N^{+} bondings formed between famotidine molecules and carboxylic groups in the mesostructure cause the delayed famotidine release rate. Such a similar delayed effect has been discussed in the reported paper [13], in which the delayed drug release effect is partially attributed to the coulombic interaction between the protonated aminopropyl groups in the mesostructure and the carboxylate anions of ibuprofen.

For the insoluble porous carrier material, the drug release kinetics is frequently described using the Higuchi model [35] expressed as follows:

$$Q_t = Kt^{1/2}, \quad (2)$$

where Q_t is the amount of drug released at release time t, K is the release rate constant for the Higuchi model.

The insets in Fig. 8 show that there are good correlation between Q_t and $t^{1/2}$ for the initial release of 60% of the adsorbed famotidine according to the Eq. (2). However, the obvious deviation from linearity can be observed after the release of 60% of the adsorbed famotidine in all the investigated release profiles. Very possibly, this kind of deviation would be linked to the dissolution of silica carriers, as discussed in Ref. [16]. In addition, the similar deviation from linearity after release of about 60% of the adsorbed drug has been found by several research groups [16,19,20], regardless of the carriers of MCM-41 or SBA-15 and regardless of the drugs of ibuprofen or gentamicin. Maybe, the deviation from overall linearity is general for the drug delivery from mesoporous materials.

4. Conclusions

It has been shown that the adsorption capacities of the carboxylic-modified mesoporous silica MSU materials for famotidine are mainly depended on the functionalization levels of carboxylic groups. In vitro release of famotidine in carboxylic-modified MSU material shows obvious delayed effect when compared with famotidine dissolution under the same conditions. The famotidine release kinetics can be controlled by the carrier effect of the carboxylic-modified MSU mesostructure and by the choice of the release solutions. Therefore, this work provides a new possibility that the potential application of carboxylic-modified mesoporous silica MSU in controlled delivery for alkaline drug molecule.

Acknowledgment

This work was supported by the Chinese National Key Basic Research Special Foundation (Grant no. 2000048001).

References

[1] A. Rivera, A. Lam, Stud. Surf. Sci. Catal. 135 (2001) 373.
[2] A. Dyer, S. Morgan, P. Wells, C. Williams, J. Helminthol. 74 (2000) 137.
[3] K.A. Fisher, K.D. Huddersman, M.J. Taylor, Chem. Eur. J. 9 (2003) 5873.
[4] J.S. Beck, J.C. Vartuli, W.J. Roth, M.E. Leonowicz, C.T. Kresge, K.D. Schmitt, C.T.W. Chu, D.H. Olson, E.W. Sheppard, S.B. McCullen, J.B. Higgins, J.L. Schlenker, J. Am. Chem. Soc. 114 (1992) 10834.
[5] D. Zhao, J. Feng, Q. Huo, N. Melosh, G.H. Fredrickson, B.F. Chmelka, G.D. Stucky, Science 279 (1998) 548.
[6] S.S. Kim, W. Zheng, T.J. Pinnavaia, Science 282 (1998) 1302.
[7] Y.-J. Han, G.D. Stucky, A. Butler, J. Am. Chem. Soc. 121 (1999) 9897.
[8] S. Murata, H. Hata, T. Kimura, Y. Sugahara, K. Kuroda, Langmuir 16 (2000) 7106.
[9] C.H. Lei, Y.S. Shin, J. Liu, J.A. Ckerman, J. Am. Chem. Soc. 124 (2002) 11242.
[10] J. Fan, C. Yu, F. Gao, J. Lei, B. Tian, L. Wang, Q. Luo, B. Tu, W. Zhou, D. Zhao, Angew. Chem. Int. Ed. 42 (2003) 3146.
[11] H.H.P. Yiu, P.A. Wright, N.P. Botting, Microporous Mesoporous Mater. 44–45 (2001) 763.
[12] M. Vallet-Regí, A. Rámila, R.P. del Real, J. Pérez-Pariente, Chem. Mater. 13 (2001) 308.
[13] B. Muñoz, A. Rámila, J. Pérez-Pariente, I. Díaz, M. Vallet-Regí, Chem. Mater. 15 (2003) 500.
[14] P. Horcajada, A. Rámila, J. Pérez-Pariente, M. Vallet-Regí, Microporous Mesoporous Mater. 68 (2004) 105.
[15] C. Tourné-Péteilh, D. Brunel, S. Bégu, B. Chiche, F. Fajula, D.A. Lerner, J.-M. Devoisselle, New J. Chem. 27 (2003) 1415.
[16] J. Andersson, J. Rosenholm, S. Areva, M. Lindén, Chem. Mater. 16 (2004) 4160.

[17] S.J. Son, J. Reichel, B. He, M. Schuchman, S.B. Lee, J. Am. Chem. Soc. 127 (20) (2005) 7316.
[18] W. Zhao, J. Gu, L. Zhang, H. Chen, J. Shi, J. Am. Chem. Soc. 127 (25) (2005) 8916.
[19] Y. Zhu, J. Shi, Y. Li, H. Chen, W. Shen, X. Dong, Microporous Mesoporous Mater. 85 (2005) 75.
[20] A.L. Doadrio, E.M.B. Sousa, J.C. Doadrio, J. Pérez Pariente, I. Izquierdo-Barba, M. Vallet-Regí, J. Control. Release 97 (2004) 125.
[21] M. Vallet-Regí, J.C. Doadrio, A.L. Doadrio, I. Izquierdo-Barba, J. Pérez-Pariente, Solid State Ion. 172 (2004) 435.
[22] M. Vallet-Regí, I. Izquierdo-Barba, A. Rámila, J. Pérez-Pariente, F. Babonneau, J.M. González-Calbet, Solid State Sci. 7 (2005) 233.
[23] G.G. Ferenczy, L. Párkányi, J.G. Ángyán, A. Kálmán, B. HegedŰs, J. Mol. Struct. (Theochem) 503 (2000) 73.
[24] Q. Tang, N. Yu, Z. Li, D. Wu, Y. Sun, Stud. Surf. Sci. Catal. 156 (2005) 649.
[25] S.A. Bagshaw, E. Prouzet, T.J. Pinnavaia, Science 269 (1995) 1242.
[26] Y.J. Gong, Z.H. Li, D. Wu, Y.H. Sun, F. Deng, Q. Luo, Y. Yue, Microporous Mesoporous Mater. 49 (2001) 95.
[27] D.J. Macquarrie, Chem. Commun. (1996) 1961.
[28] J.A. Elings, R. Ait-Meddour, J.H. Clark, D.J. Macquarrie, Chem. Commun. (1998) 2707.
[29] N. Liu, R.A. Assink, C.J. Brinker, Chem. Commun. (2003) 370.
[30] T. Kokubo, H. Kushitani, S. Sakka, T. Kitsugi, T.J. Yamamuro, Biomed. Mater. Res. 24 (1990) 721.
[31] X.S. Zhao, G.Q. Lu, J. Phys. Chem. B 102 (1998) 1556.
[32] F. de Juan, E. Ruiz-Hitzky, Adv. Mater. 12 (2000) 430.
[33] A. Shimojima, N. Umeda, K. Kuroda, Chem. Mater. 13 (2001) 3610.
[34] M. Jia, A. Seifert, W.R. Thiel, Chem. Mater. 15 (2003) 2174.
[35] T. Higuchi, J. Pharm. Sci. 52 (1963) 1145.